Contrast Driven Elastica for Image Segmentation

Noha Youssry El-Zehiry, *Member, IEEE*, and Leo Grady, *Member, IEEE*

***Abstract*— Minimization of boundary curvature is a classic regularization technique for image segmentation in the presence of noisy image data. Techniques for minimizing curvature have historically been derived from gradient descent methods which could be trapped by a local minimum and, therefore, required a good initialization. Recently, combinatorial optimization techniques have overcome this barrier by providing solutions that can achieve a global optimum. However, curvature regularization methods can fail when the true object has high curvature. In these circumstances, existing methods depend on a data term to overcome the high curvature of the object. Unfortunately, the data term may be ambiguous in some images, which causes these methods also to fail. To overcome these problems, we propose a contrast driven elastica model (including curvature), which can accommodate high curvature objects and an ambiguous data model. We demonstrate that we can accurately segment extremely challenging synthetic and real images with ambiguous data discrimination, poor boundary contrast, and sharp corners. We provide a quantitative evaluation of our segmentation approach when applied to a standard image segmentation data set.**

***Index Terms*— Euler elastica, weighted curvature, combinatorial optimization, primal formulation, image segmentation.**

I. Introduction

A CLASSIC approach to image segmentation is to formulate the problem as an energy minimization problem

$$E = E_{\text{data}} + E_{\text{boundary}}, \tag{1}$$

where E_{data} models the object and background appearance (intensity, color, texture, etc.) and E_{boundary} models the boundary of the object. The principle behind this model is that the data term may be noisy or ambiguous, and therefore the boundary model can be used as a *regularization* to overcome this noise or ambiguity.

A classic prior model for the boundary of objects is the elastica model which models the object boundary as having short length and low curvature. This model was proposed and theoretically justified by Mumford [20] and also appeared in the first active contour work by Kass *et al.* [16] who proposed an optimization of the boundary curvature. Subsequently, the optimization of boundary curvature became a common feature of variational methods for active contours and level sets [7], [12], [27]. However, all of these methods use descent-based optimization, causing the solution to get stuck in a local minimum and depend strongly on having a good initialization. This dependence on initialization (and speed of the curvature optimization) have caused many researchers to abandon the curvature term, particularly after combinatorial and convex optimization methods became popular for producing global optima of the data and boundary length terms. Beyond the elastica model, curvature regularization has appeared in several forms in the computer vision literature, of which Mumford's elastica model is just one example. Other approaches use cycle ratios to provide curvature dependent image segmentation [15], [24]. Schoenemann *et al.* presented globally optimal image segmentation by minimizing the ratio of the flux over the weighted sum of length and curvature of the object of interest. However, the memory requirements and the computational time of this approach makes it impractical for many vision applications.

Following the description by Bruckstein *et al.* [6] of the curvature of a polygon, the curvature of an object boundary was formulated on a graph by Schoenemann *et al.* [25] (and previously in a different manner by the same authors [24]) such that combinatorial optimization methods could be applied to optimize curvature. Specifically, on the graph *dual* to the pixel lattice, the boundary of an object may be described by a polygon comprised of graph edges, and therefore the boundary having minimum curvature could be found by optimizing over all polygons which had a curvature value as defined by Bruckstein *et al.*. The optimization has been performed by casting the curvature formulation into an Integer Linear Programming (ILP) problem that assigns an indicator function to the edges of the polygon. However, this optimization required a long computation time (minutes to hours) and often did not find a solution achieving a global optimum. The same optimization framework has been used by Strandmark and Kahl *et al.* [30]. The work of Schoenemann *et al.* [25] was followed by El-Zehiry and Grady [10] who used a *primal* formulation of the curvature energy that parameterized a space of boundary polygons in terms of the normal vectors defined by lattice edges and computed a solution in seconds which often achieved a global optimum. For simplicity, in this work we consider only the segmentation of an object from a background, i.e., a two-class image segmentation problem.

A major problem with the segmentation model in (1) is the assumption that the data term is mostly unambiguous and therefore strong enough to overcome objects which do

Manuscript received October 16, 2014; revised May 24, 2015; accepted November 19, 2015. Date of publication March 23, 2016; date of current version April 14, 2016. This work was completely developed when Dr. Grady was with Siemens. The associate editor coordinating the review of this manuscript and approving it for publication was Dr. Yonggang Shi. *(Corresponding author: Noha Youssry El-Zehiry.)*

N. Y. El-Zehiry is with Siemens Healthcare, Princeton, NJ 08540 USA (e-mail: noha.el-zehiry@siemens.com).

L. Grady was with Siemens, Princeton, NJ 08540 USA. He is now with HeartFlow Inc., Redwood City, CA 94063 USA (e-mail: leograd@yahoo.com).

Color versions of one or more of the figures in this paper are available online at http://ieeexplore.ieee.org.

Digital Object Identifier 10.1109/TIP.2016.2545244

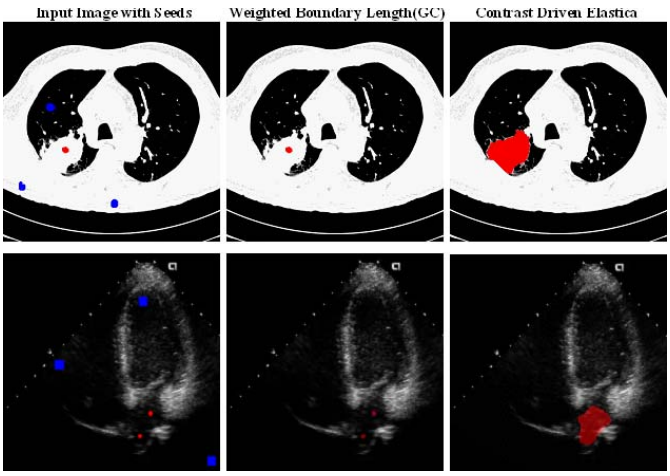

Fig. 1. Two segmentation problems with an ambiguous data term as a result of the object interior and substantial parts of the exterior sharing the same distribution. User-provided object/background seeds are shown as red and blue dots in the first column. First row: Segmentation of a lung tumor in a chest CT scan. Graph cuts (weighted boundary length regularization) produced a trivial segmentation around the foreground seed due to the poor data term and poor boundary definition. Our contrast driven elastica model correctly classified the pixels. Second row: Segmentation of the left atrium. Again, graph cuts produced a trivial segmentation around the foreground seed due to the poor data term and poor boundary, but our contrast driven elastica provides the correct segmentation.

not fit the boundary model. For example, sharp corners in a medical images have both long boundary length and high curvature, which means that the data term in (1) would have to be strong in order to avoid having the regularization influence the segmentation toward an incorrect short boundary length and low curvature segmentation. To avoid this problem for the boundary length model, the geodesic active contours [7] and weighted Graph Cuts [4] models were introduced, which accommodated poor data terms by *weighting* the boundary length regularization in areas of high contrast. Effectively, these approaches allowed for objects with long boundary length, as long as the boundary contrast was high. Unfortunately, no such improvement has been proposed to accommodate objects with high curvature. Due to the recent improvements in optimization of the full elastica model (including the curvature term), we propose a *contrast driven* elastica model which allows objects to possess a high curvature if the boundary contrast supports this conclusion. Using our contrast driven elastica model, we can segment objects with high boundary curvature even when the data term is ambiguous or poorly defined. Figure 1 gives an example of a segmentation problem with poor data term definition (since the object and some of the background have an identical distribution), for which the curvature term is necessary to obtain a quality segmentation.

One method which has been used in past to address the unreliability of a data term is to interactively incorporate user-defined *seeds*; a foreground seed is a small subset of pixels that have been labeled as belonging to object and a background seed is a small subset of pixels that have been labeled as belonging to background. These seeds may be obtained interactively from a user who is specifying a particular object (e.g., [4], [22]) or automatically from a system trained to look for a particular object (e.g., [13], [32]). For example, this type of approach which uses seeds and contrast-sensitive edge weighting has been employed with such popular algorithms as Graph Cuts [4], Random Walker [14], geodesic segmentation [2] and power watersheds [9]. However, since curvature is a function of triple-cliques it is much less clear how to use traditional contrast weighting for a curvature regularization model. Seeds may also be incorporated into our contrast driven elastica method to interactively specify regions with poor data term definition. As shown in Figure 1, our use of a contrast driven elastica regularization is much more powerful than the standard length regularization even in an interactive setting, since it requires many fewer user interactions.

Most of the current curvature regularization models [10], [21], [25], [30], [34] assume an unambiguous data term that provides enough discrimination between the object and the background. Our contrast driven elastica regularization model does not have this constraint and works efficiently whether a good data term exists or not. To the best of our knowledge, we were the first to introduce a contrast weighted curvature regularization model [11]. In 2013, Krueger et *al.* [19] introduced a weighted pseudo-elastica model that is aiming at optimizing an approximation of curvature and it incorporated edge weights in a similar fashion to Geodesic Active Contours (GAC) [7]. Unlike our region based curvature regularization model, the approach presented in [19] is an edge based model that requires the user's interaction to be on the boundary of the object of interest. Comparison with edge based approaches are beyond the scope of this paper. However, we highlight the main differences between [19] and our current contribution.

First: our elastica model builds upon the Bruckstein discrete representation of curvature in [6] which converges to the continuous notion of curvature if the graph resolution is increased. The pseudo elastica model only presents an approximation of curvature that does not converge to continuous curvature even for finer grids. Moreover, to preserve a low computational complexity, the optimization in [19] involves many heuristics that result in an approximate suboptimal solution rather than a global solution which we guarantee at least for 4-connected grids.

Second: The pseudo-elastica model in [19] inherits all the disadvantages of the edge based segmentation approaches, and on the top of them, the inability to handle topology changes in the object of interest. In other words, the final boundary must be a continuous boundary representing the minimal curvature path between the initial seed points defined by the user's interaction.

Finally, the seeds must be placed on the boundary itself which is quite challenging. It requires accurate localization of the seed points as any small deviation in the seeds may lead to a shift in the whole boundary resulting in inaccuracies in any quantitative measures that are dependent on the segmentation accuracy (e.g. organ size, tumor shape descriptors, ..etc). Moreover, placing the seeds on the boundary makes it harder to automate the seed generation step which can be easily done if rough brush seeds are used inside and outside the object of interest.

The advantage of the pseudo-elastica approach in [19] is that it can handle open contours which cannot be easily done using our region based weighted curvature regularization method. This was illustrated by the filament example in [19, Fig. 9].

The rest of the paper is organized as follows: In Section II, we build our contrast driven elastica model on the fast algorithm introduced in [10]. In Section III, we test the model with several experiments, including quantitative assessment on a known database and a qualitative assessment on images which were selected to highlight the strength of our model over all known approaches. Finally, in Section IV we draw conclusions and suggest future directions.

II. Methods

We begin this section with a short review of the elastica optimization method presented in [10] before proceeding to our generalized contrast driven elastica formulation, optimization and results.

A. Contrast Driven Elastica Energy

The continuous formulation of Mumford's Elastica model is defined for curve $\mathcal{C}$ as

$$E(\mathcal{C}) = \int_{\mathcal{C}} (a + b\kappa^2) ds \quad a, b > 0, \tag{2}$$

where κ denotes the scalar curvature and ds represents the arc length element. When $a = 0$ (the arc length is ignored), the model reduces to the integral of the boundary squared curvature $E(\mathcal{C}) = \int_{\mathcal{C}} \kappa^2 ds$. The combinatorial optimization of a discrete form of this model (in which boundary polygons are mapped to cuts) has been presented in [10]. We now review the main points of this formulation.

1) Curvature Energy: The use of combinatorial optimization to minimize the elastica model prompted the discrete formulation of the curvature on a graph. A graph $\mathcal{G} = \{\mathcal{V}, \mathcal{E}\}$ consists of a set of vertices $v \in \mathcal{V}$ and a set of edges $e \in \mathcal{E} \subseteq \mathcal{V} \times \mathcal{V}$. An edge incident to vertices v_i and v_j is denoted e_{ij}. In our formulation, each pixel is identified with a node, v_i. A weighted graph is a graph in which every edge e_{ij} is assigned a weight w_{ij}. An edge cut is any collection of edges that separates the graph into two sets, $\mathcal{S} \subseteq \mathcal{V}$ and $\overline{\mathcal{S}}$, which may be represented by a binary indicator vector x,

$$x_i = \begin{cases} 1 & \text{if } v_i \in \mathcal{S}, \\ 0 & \text{else.} \end{cases} \tag{3}$$

The cost of the cut represented by any x is given by

$$\text{Cut}(x) = \sum_{e_{ij}} w_{ij} |x_i - x_j|. \tag{4}$$

Bruckstein *et al.* [6] expressed the curvature of a 2D polygon in terms of the angular change between consecutive polygonal segments. Instead of a polygon, it was observed in [25] that the polygon could be viewed as existing on a *dual* graph. However, in [10] the idea of optimizing the curvature of polygons normal to the edge sets was formulated on a *primal* graph in order to permit an easier optimization and more generalizable formulation. In this formulation, if two edges e_{ij} and e_{ik}, incident to a node v_i, are cut then the cut is penalized with value

$$w_{ijk} = \frac{\alpha^p}{\min(|\overrightarrow{e_{ij}}|, |\overrightarrow{e_{ik}}|)}, \tag{5}$$

where α is the angle between the edges. Consequently, each cut in the graph is associated with a polygon for which the Bruckstein curvature can be measured and these curvature measurements can be optimized. In the remainder of this manuscript, we use the term *curvature* to indicate the Bruckstein curvature of the boundary polygons associated with each cut.

Specifically, it was shown in [10] that the triple clique representing angular change in the boundary polygon can be exactly decomposed into three edge weights

$$E(x_i, x_j, x_k) = w_{ij}|x_i - x_j| + w_{ik}|x_i - x_k| - w_{jk}|x_j - x_k|, \tag{6}$$

where $w_{ij} = w_{ik} = w_{jk} = \frac{1}{2} w_{ijk}$.

Therefore, the minimum cut with respect to these edge weights is a cut that finds the associated polygon with minimal Bruckstein curvature. Despite the nonsubmodularity of the curvature energy in (6), it was shown in [10] that Quadratic Pseudo Boolean Optimization (QPBO) and Quadratic Pseudo Boolean Optimization with Probing (QPBOP) are able to find a minimum cut in most circumstances. Notice that although the curvature clique was designed to penalize the cut of both edges e_{ij} and e_{ik}, the decomposition to pairwise interactions introduces an edge e_{jk} with negative weight. We denote the set of effective edges (the set of original graph edges in union with the set of these introduced edges) as $\mathcal{E}^* \supseteq \mathcal{E}$.

2) Planar Versus Nonplanar Graphs: The formulation on the primal graph in [10] is exactly equivalent to the original formulation presented by Schoenemann in [25] when a planar graph is used (*i.e.* the dual exists). This holds only for 4-connected lattices that may present metrication artifacts. However, 8-connected graphs are nonplanar and hence have no dual. In this paper, we propose to planarize the 8-connected lattice by adding auxiliary nodes. Any nonplanar graph can be planarized as follows:

1) Find all the edge crossings in the nonplanar graph.
2) Planarize the nonplanar graph by adding an auxiliary node at each edge crossing.

Figure 2 shows the nonplanar 8-connected lattice and the corresponding planarized lattice created by adding an auxiliary vertex at the crossing of the diagonal edges. Hence, the curvature formulation in [10] can be used for the planarized lattice in Figure 2 (b).

3) Weighted Curvature Energy: The formulation presented above from [10] places a strong penalty on boundaries which have a high curvature, even if that curvature is well-supported by the boundary contrast. Specifically, each edge pair above is associated with an angle in the boundary polygon. Therefore, we propose to relax the penalty associated with a sharp angle when the angle is well-supported with boundary contrast by *weighting* the corner (edge pair) to reflect the boundary contrast. Traditional contrast edge weighting formulas have been constructed in terms of node

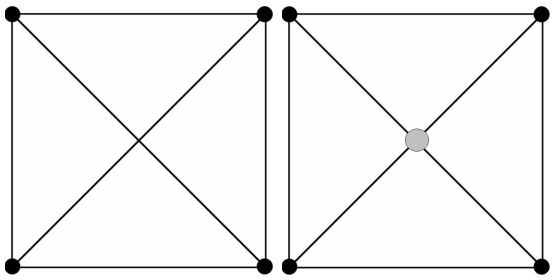

(a) (b)

Fig. 2. 8 point nonplanar graph may be planarized by inserting an auxiliary node at each edge crossing of a nonplanar graph. (a) Nonplanar 8-connected lattice, (b) Planarized lattice with auxiliary nodes (in gray) inserted at every edge crossing.

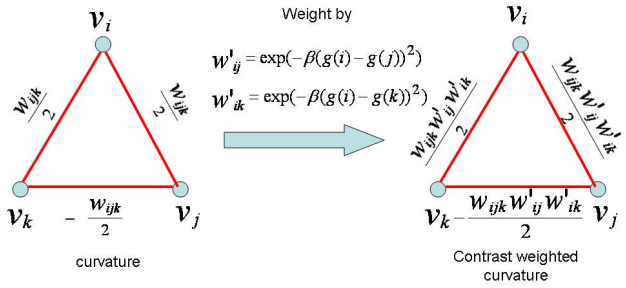

Fig. 3. Weighted versus unweighted curvature cliques.

pairs (corresponding to an edge). It is much less clear how to construct a contrast-weighting formula for the type of node triple-clique that forms the basis of the curvature formulation in [10].

According to the curvature formulation in [10], edges e_{ij} and e_{ik} are cut when the pixel i is a foreground pixel and j and k are background pixels or vice versa. Therefore, we propose to weight the curvature clique formed by these edges by the appearance differences between pixels i and j and the appearance difference between i and k. This can be formulated as follows: Given a 2D image with image values associated with each pixel (node), $g : \mathcal{V} \rightarrow R$. The weighted curvature penalty w^*_{ijk} is given by

$$w^*_{ijk} = w_{ijk}\, w'_{ij}\, w'_{ik}, \tag{7}$$

where we can use a typical contrast weighting function for the pairwise edges [4], [28], such as

$$w'_{ij} = \exp(-\beta(g(i) - g(j))^2), \tag{8}$$

and

$$w'_{ik} = \exp(-\beta(g(i) - g(k))^2), \tag{9}$$

where $g(i)$, $g(j)$ and $g(k)$ represent the image intensities at pixels v_i, v_j and v_k, respectively and β is a free parameter controlling the contrast strength. The triple weighted curvature clique can be decomposed, similar to the unweighted case, into three edge weights yielding

$$E(x_i, x_j, x_k) = w^*_{ij}|x_i - x_j| + w^*_{ik}|x_i - x_k| - w^*_{jk}|x_j - x_k|, \tag{10}$$

where $w^*_{ij} = w^*_{ik} = w^*_{jk} = \frac{1}{2}w^*_{ijk}$. This weighting construction is illustrated in Figure 3.

Note that we view gradients in image intensity as just one illustrative model. More advanced contrast weighting could also be used which applies differences in color, texture or other higher-order features.

4) Boundary Length Energy: The second term in the elastica energy of (2) is the boundary length term. The boundary length term corresponds to the minimum cut term in graph-based methods, which identifies the boundary length with a cut using edge weights which may be weighted to reflect Euclidean boundary length [5].

The boundary length energy is represented by

$$E_{\text{length}}(x) = \sum_{e_{ij} \in \mathcal{E}^*} w_{ij}\,|x_i - x_j|, \tag{11}$$

where the boundary length weight w_{ij} could be set to $w_{ij} = w'_{ij}$ (as in [4] and [7]), $w_{ij} = 1$ or to reflect Euclidean boundary length (as in [5]). Note that despite the similarity of (10) and (11), the weighting (particularly the negative weighting) distinguishes the role of these terms into a penalty of boundary length or the Bruckstein curvature of the associated polygon. However, the ability to write both terms as a cut is what makes it possible (here and in [10]) to perform the optimization efficiently.

5) Summary: The segmentation problem is modeled as the solution, x, which minimizes the energy

$$E(x) = E_{\text{data}}(x) + \lambda E_{\text{length}} + \nu E_{\text{curvature}}(x) \tag{12}$$

for positive weighting parameters ν and λ that control the strength of the boundary length term and boundary curvature term, respectively.

In our experiments, we use a simplistic data term (e.g., Chan-Vese data model [8]) to illustrate our method. This data term is given by

$$E_{\text{data}}(x) = \sum_{v_i \in \mathcal{V}} x_i\,(g(i) - \mu_F)^2 + \sum_{v_i \in \mathcal{V}} (1 - x_i)\,(g(i) - \mu_B)^2\,, \tag{13}$$

where $g(i)$ is the image intensity at the pixel v_i, the values of μ_F and μ_B represent the mean intensity values of the model intensities for object (foreground) and background. If the data term does not provide informative discrimination between the foreground and background (i.e., $\mu_F \sim \mu_B$, see examples in Figure 4), then the term is effectively removed from the energy, leaving only the regularization terms to find the appropriate segmentation.

The curvature term is written as a summation by

$$E_{\text{curvature}}(x) = \sum_{e_{ij} \in \mathcal{E}^*} w^*_{ij}\,|x_i - x_j|, \tag{14}$$

where w^*_{ij} reflects the contrast weighted curvature penalty and is calculated from (7) and (8).

The boundary length term is given by (11). Foreground and background seeds may also be used to constrain

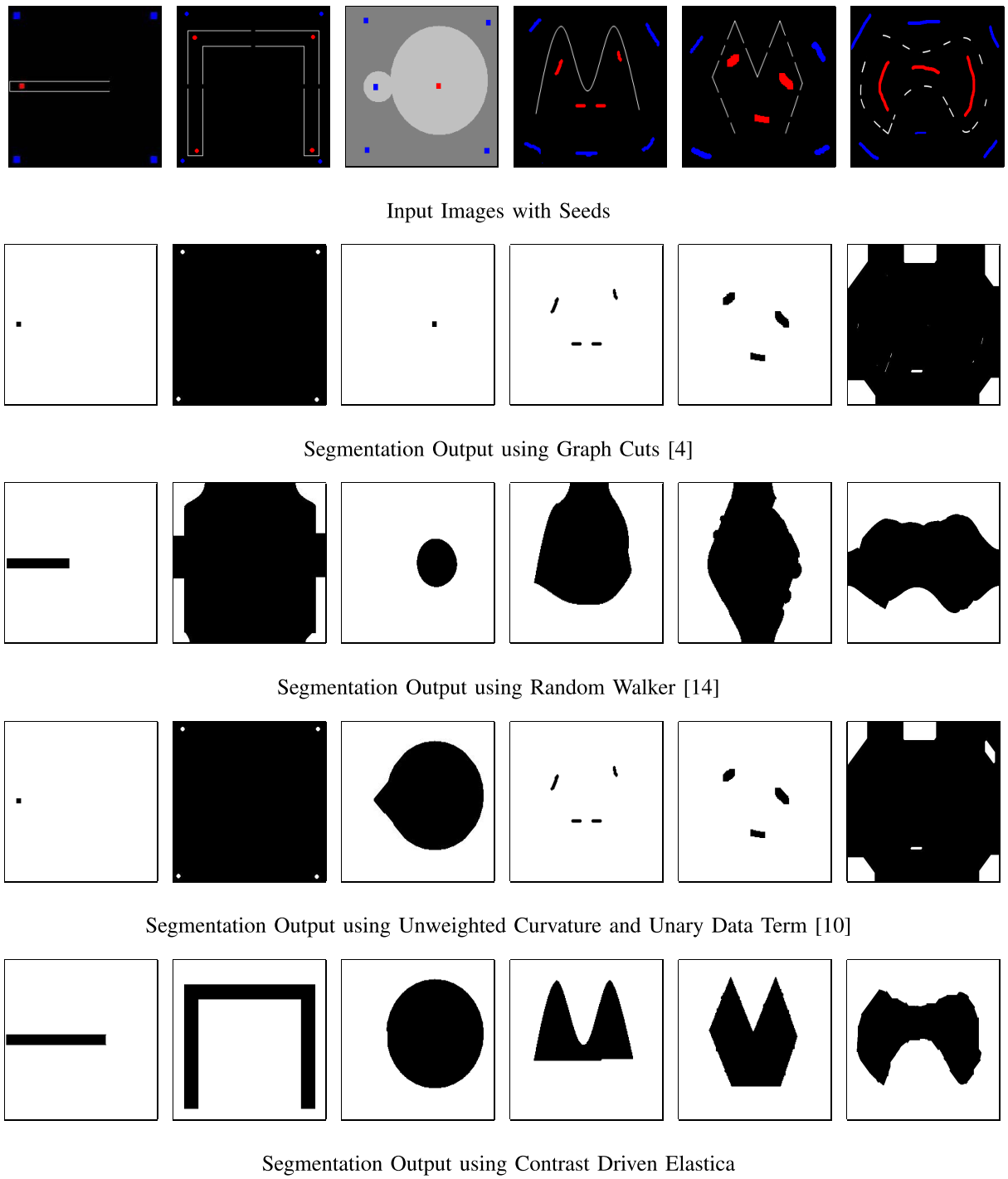

Fig. 4. Segmentation of synthetic images with identical foreground and background intensity profiles, weak object boundaries and irregular shapes. Comparison of segmentation results via weighted boundary length (Graph Cuts) [4], Random Walker [14], unweighted curvature [10] and our contrast driven elastica method.

the segmentation. A foreground seed v_i is set to $x_i = 1$ while a background seed is set to $x_i = 0$.

B. Optimization

In [10] and in our contrast driven formulation, the elastica problem was transformed into the problem of finding a minimum cut on a graph in which some of the edge weights were negative. Unfortunately, the third term of (6) violates the submodularity constraint and causes the minimum cut problem to be nonsubmodular [18], *i.e.*, straightforward max-flow/min-cut algorithms will not yield a minimum cut. However, it was shown in [10] that the Quadratic Pseudo Boolean Optimization (QPBO) [17] and Quadratic Pseudo Boolean Optimization with Probing (QPBOP) [23] offered a solution to the optimization problem that frequently offered a complete, optimal solution.

The QPBO technique has the remarkable ability to provide a partial labeling of the variables which is *optimal* for all

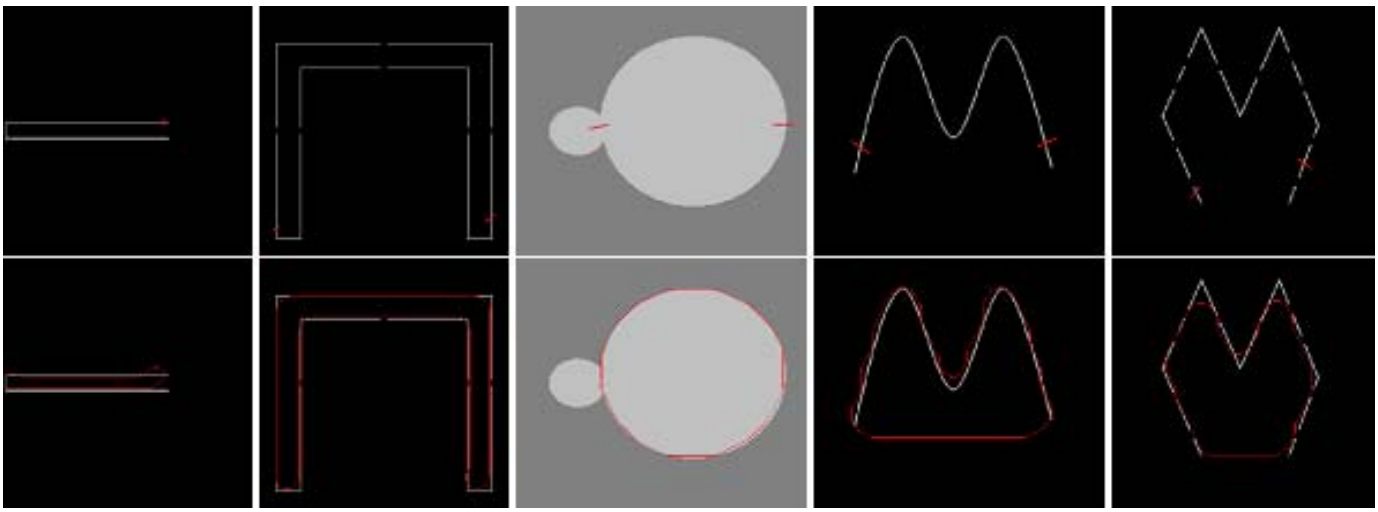

Fig. 5. Results of the weighted pseudo elastica segmentation approach [19] on the challenging synthetic images with no appearance discrimination between the object of interest and the background.

labeled variables. The output of QPBO is

$$x_i = \begin{cases} 1 & \text{if } v_i \in \mathcal{S}, \\ 0 & \text{if } v_i \in \overline{\mathcal{S}}, \\ \emptyset & \text{otherwise.} \end{cases} \tag{15}$$

Recall that $\mathcal{S}$ represents the set of nodes that minimizes our discrete elastica energy.

Theoretically, an ambiguous data model (unary term or terminal links in the graph) may cause the optimization scheme using QPBO/QPBOP (used in [10]) to be more challenging and to provide an incomplete labeling. However, a sufficiently high λ makes the problem submodular and hence exactly solvable. In all of our experiments, despite using a smaller λ[1] (for which the problem was still nonsubmodular), QPBOP succeeded to provide a complete solution and thus a global optimum of the contrast driven elastica model.

III. Experimental Results

The motivation for our contrast driven elastica algorithm was to employ higher-order (curvature) regularization for objects with sharp corners, even in the presence of ambiguous or poorly-defined data terms. Therefore, we must verify that our contrast-weighting modification allows us to segment objects with high curvature and poor data term differentiation with respect to both a contrast weighted boundary length regularization (i.e., graph cuts) and an unweighted curvature regularization. Additionally, we must verify that our modification of the elastica model does not cause it to behave poorly on images with a good data term differentiation. We start by demonstrating the strength of our model on synthetic and real examples of images with poor data term definition and images with sharp corners and complex boundaries. We show that our contrast driven elastica algorithm is far superior to the boundary length and unweighted curvature models. We then proceed to present a quantitative comparison by applying our model to a standard image segmentation database and to show that it performs as good or better than existing algorithms on this database, even though the data terms are relatively informative.

[1]We used a smaller λ because a very high value of λ would make the length term much more dominant and would diminish the effect of the curvature term.

A. Images With Poor Data Term Differentiation

In order to illustrate the difficulty associated with high curvature objects and poor data term differentiation, we first created some synthetic images which were designed to highlight three major challenges: 1) Ambiguity of data term (*i.e.*, object and background share the same intensity profile), 2) Incomplete boundaries, 3) Accurate segmentation of high curvature features such as cusps and sharp corners.

Figure 4 shows six synthetic images in which an appearance term is not useful to define a segmentation and for which the object boundaries are incomplete and the shapes are irregular. Such images present a strong challenge to existing algorithms which rely on appearance descriptions and a model of short boundary length. For each image, we provide the results of our proposed approach and a comparison with other segmentation approaches typically used to segment such images. Segmentation results for weighted boundary length (Graph Cuts) [4], random walker segmentation [14] and unweighted curvature segmentation [10] is presented. For the unweighted curvature with unary data terms, μ_F and μ_B are calculated as the mean values for the foreground and background seeds as suggested in [10].

Ambiguity of the data term is illustrated in the synthetic examples we created in Figure 4, the foreground and background in these images share the same intensity profile. Weighted boundary length segmentation favors the cut with the minimum number of edges resulting is a trivial solution around the seeds. Random Walker works, intuitively, by calculating the probability that a random walk starting at a particular pixel will first reach one of the seeds. Hence, it suffers from a proximity problem that results in a premature stopping because

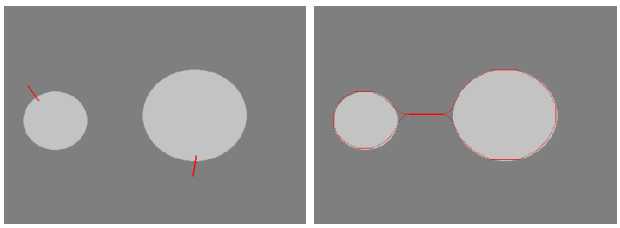

Segmentation of disconnected objects using the pseudo elastica.

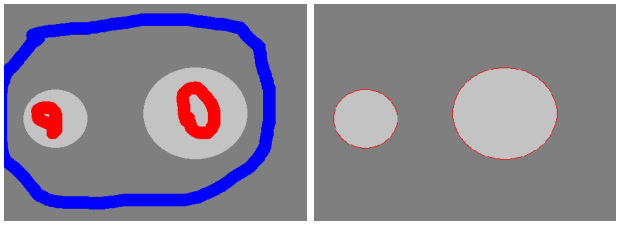

Segmentation of disconnected objects using our approach.

Fig. 6. Comparison of the weighted pseudo elastica to our algorithm in segmenting disconnected objects.

a random walk from an erroneously-background-labeled pixel would have a higher probability reaching the background seeds than the foreground one producing an undersegmented object as illustrated by the result of the first and third images. Unweighted curvature regularization also fails to provide a proper segmentation. Since the unary data term does not provide any discrimination in the first image, the minimum curvature is obtained by assigning all the image to one class except for the seeds of the other class. Our contrast driven elastica approach provides the correct segmentation as it extends the seeds due to strong contrast at the boundary. When the boundary information is missing such as the gaps in the second image and last closed polygons, the elastica model favors to bridge these gaps and produce a connected object because disconnecting them will result in a boundary of higher curvature.

Incomplete boundaries such as the open polygons depicted in the fourth and fifth input images of Figure 4 also challenge the Random Walker due to the seed proximity, resulting in substantial leakage through the large gaps. In comparison, the contrast driven elastica seamlessly bridges these gaps in the sense that it minimizes the curvature connecting the end points of the polygons with straight segments. The same images feature high curvature structures such as cusps. However, due to the contrast present at these features, our algorithm is capable to fit them precisely.

A notable contribution that was not included in the comparison in Figure 4 is the weighted pseudo-elastica model presented in [19]. As discussed previously, comparison to edge based methods is beyond the scope of this paper. However, we provide in Figure 5 the results obtained using the weighted pseudo elastica on the challenging images with no data discrimination to illustrate how to it compares to our algorithm. In [19], the algorithm requires user interaction by drawing two strokes that intersect the boundary of the object

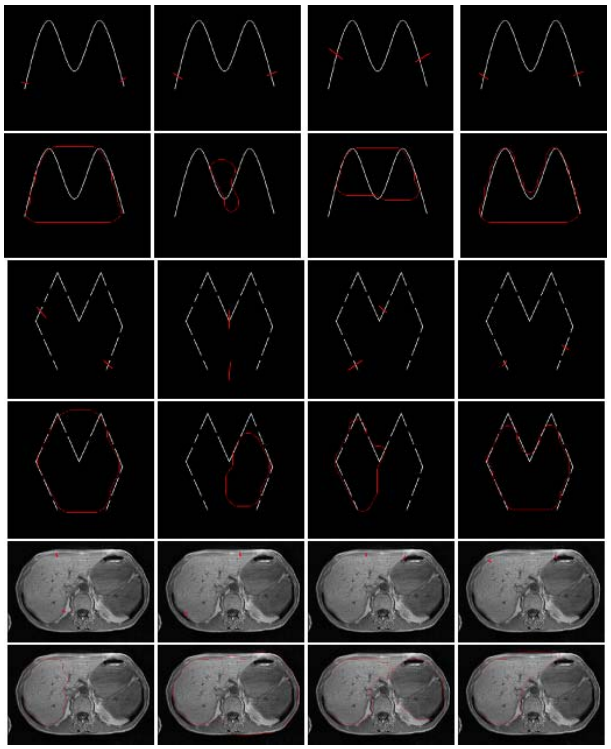

Fig. 7. Sensitivity to the initialization for the pseudo elastica segmentation algorithm in [19].

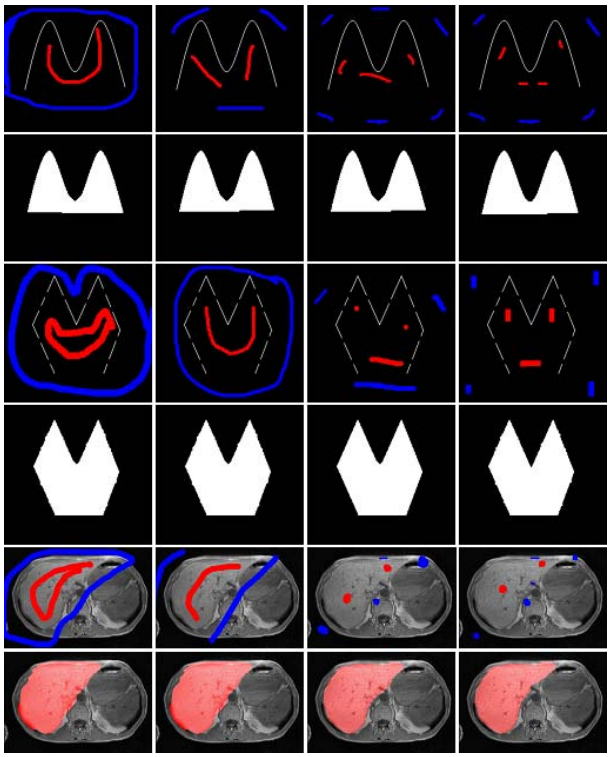

Fig. 8. Sensitivity to the initialization for our algorithm.

of interest rather than strokes inside and outside the object of the interest. To achieve fairness, we have experimented with multiple stroke locations and tuned the parameters for the best possible results that can be obtained using the algorithm.

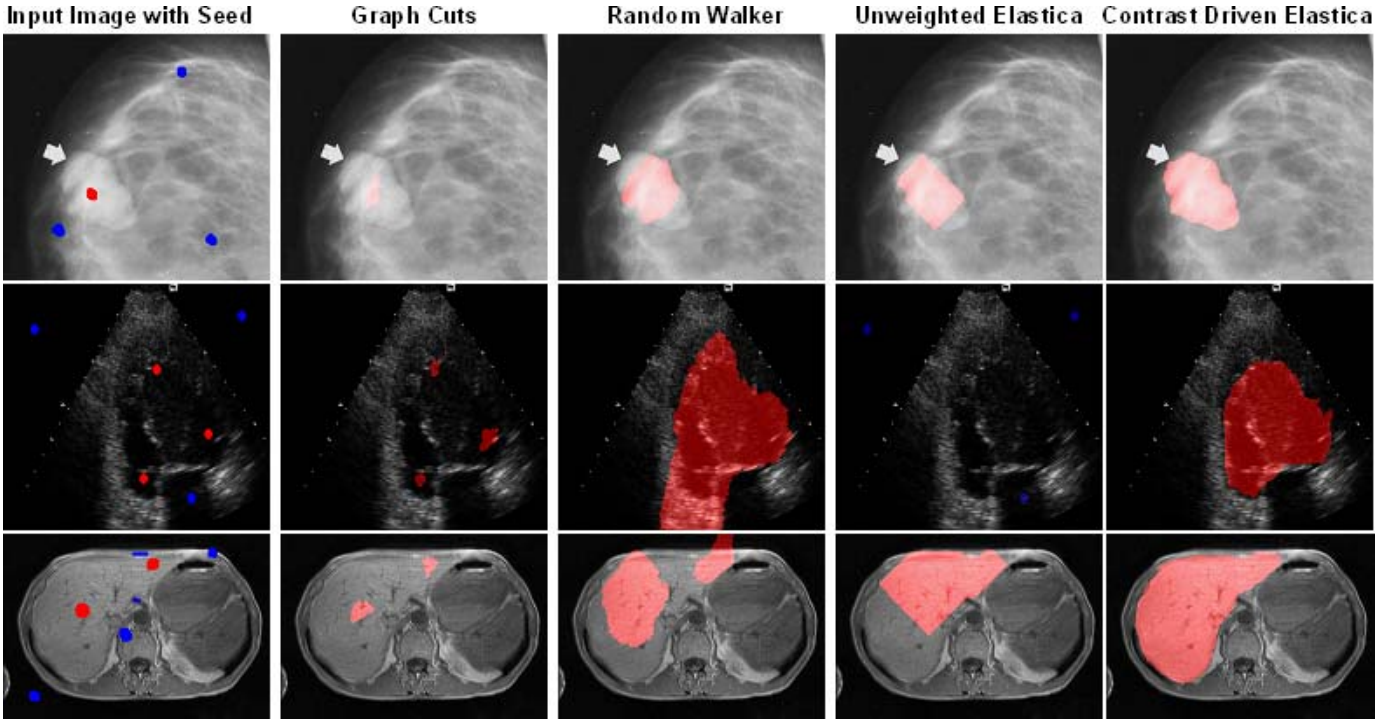

Fig. 9. Medical examples of images with ambiguous data terms, weak boundaries and limited seeds. First row: Circumscribed mass in a mammogram. Second row: Left ventricle in ultrasound. Third row: Liver in MRI. The Graph Cuts algorithm resulted in trivial solutions as a result of ambiguous data terms, few seeds and poor boundary contrast. The Random Walker algorithm exhibited over dependence on seed proximity in these ambiguous images. The unweighted curvature algorithm resulted in the minimum curvature boundary that fits the poor intensity profile provided by the seeds, producing false negatives. In comparison, our contrast driven elastica model detected the correct boundaries in all cases despite these challenging images.

The top row of Figure 5 shows the initialization of the segmentation for each image. The bottom row depicts the segmentation results obtained using the weighted pseudo elastica. The results of the second and fifth images illustrate that the sharp corners cannot be preserved very well even in the existence of sharp contrast. We found this a consistent behavior no matter how we choose the parameters. On the contrary, our weighted curvature formulation preserves the corners very accurately as long as they are supported with high contrast. Moreover, when the images get more challenging (for example missing boundaries), the algorithm fails to provide proper completion to such boundaries as shown in the first and fourth images. It is, to some extent, relevant to the corner preservation issue. Had the edge in the bottom of the fourth image not been missing, two corners would have formed. Due to the fact that the corner has a missing edge, the weighted pseudo elastica fails to properly preserve the corner and constructed a rounded, smooth corner leading to the formed bottom edge being lower than it is supposed to be.

Another aspect of the comparison to weighted Pseudo Elastica is the ability to capture topology changes correctly. The weighted pseudo elastica approach inherits the drawbacks of the edge based segmentation approaches such as the failure to provide proper segmentation in the existence of topology changes. The approach provides the boundary as a single connected component. However, our formulation is region based and intuitively handles disconnected components of a single object. Figure 6 illustrates the segmentation of an object that consists of two disconnects circles. Our algorithm seamlessly provides the correct segmentation of the circles. Conversely, the weighted pseudo elastica falsely connects the two circles.

Additionally, experimental evaluation showed that the weighted pseudo elastica is very sensitive to the placement of the initialization strokes to the extent that it may fail in some cases as depicted in Figure 7 but our algorithm is more robust to initialization as depicted in Figure 8.

B. Real Images With Ambiguous Appearance

Although the previous set of images were synthetically created to highlight challenges in image segmentation, these scenarios are actually quite common in the segmentation of real images, particularly medical images. Figure 9 demonstrates the performance of our model on some medical imaging applications and different modalities.

Ambiguity of the data term is a common feature in a variety of medical imaging segmentation problems. For example, a circumscribed mass may have the same intensity profile as the surrounding tissue, which is depicted in the first image of Figure 9. The liver and the abdominal muscles share the same intensity levels. Graph Cuts produce a trivial segmentation for these cases. The Random Walker results exhibit over dependence on the proximity of the seeds in these ambiguous situations, leading to both false positives and false negatives. The unweighted curvature algorithm produces a boundary of minimum curvature that respects the global data model derived from the seeds, but fails to provide a quality segmentation due to the poor quality of the global data model.

TABLE I

WE COMPARE OUR CONTRAST DRIVEN ELASTICA SEGMENTATION ALGORITHM TO FIVE OTHER ALGORITHMS ON THE GRABCUT DATABASE OF [3]. THE DATA TERMS IN THIS DATABASE ARE RELATIVELY INFORMATIVE AND THEREFORE ALL SIX ALGORITHMS PRODUCE QUALITY IMAGE SEGMENTATION RESULTS. OUR CONTRAST DRIVEN ELASTICA ALGORITHM PROVIDES SEGMENTATION RESULTS WHICH ARE AS GOOD OR BETTER THAN THESE ALGORITHMS ON THIS DATABASE. ADDITIONALLY, SECTIONS III-A AND III-B SHOW THAT OUR ALGORITHM STILL MAINTAINS ITS QUALITY FOR IMAGES WITH AMBIGUOUS DATA TERMS, EVEN WHEN THE OTHER ALGORITHMS ARE UNABLE TO PRODUCE QUALITY SEGMENTATION. WE DID NOT INCLUDE A COMPARISON TO THE UNWEIGHTED ELASTICA BECAUSE ALL OF THE SIX ALGORITHMS LISTED ABOVE DO NOT INCLUDE UNARY DATA TERM BUT THE UNWEIGHTED ELASTICA IN [10] DOES SO THE COMPARISON WILL NOT BE FAIR

	BE	GCE	VOI	RI
Graph Cuts	3.276	0.028	0.196	0.970
p-brush ($p = 1.25$)	3.241	0.028	0.193	0.971
p-brush ($p = 1.75$)	3.206	0.027	0.187	0.972
Random Walker	3.206	0.026	0.185	0.972
Power Watershed	2.888	0.025	0.210	0.970
Contrast Driven Elastica	2.683	0.024	0.205	0.971

Objects with weak boundaries also appear frequently in medical images. For example, the boundaries of the left atrium shown in Figure 1 or the boundaries of the left ventricle depicted in Figure 9. In both cases, the Graph Cuts and unweighted curvature algorithms yield a trivial solution due to the lack of any discriminatory power of the data term. Due to the seed proximity, the Random Walker algorithm leaks through the gaps in the boundary, resulting in an over segmented object. However, leakages are prevented using our contrast driven elastica approach because any leakages in the boundary will have a higher curvature and will produce a higher energy solution.

C. Assessment on a Database With Positive Data Differentiation

In this section, we examine whether our modified elastica model can perform well when there is a substantial differentiation in the data term. To assess this issue, we provide a quantitative comparison between the performance of our contrast driven elastica algorithm with the contrast-weighted boundary length model (Graph Cuts)[2] [4], the p- brush approach in [29] (with two different p values) the Random Walker of [14]) and the power watershed [9]. We applied the six algorithms to the set of images in the Microsoft GrabCut database used in [3]. The database contains ground truth segmentation for 50 color images corresponding to indoor as well as outdoor scenes. We quantify the results using four segmentation error measures [33]:

[2]An independent comparison of our approach in [11] versus graph cuts was done by Krueger et *al.* in [19] on very challenging medical images. They show that our model provides better segmentation results.

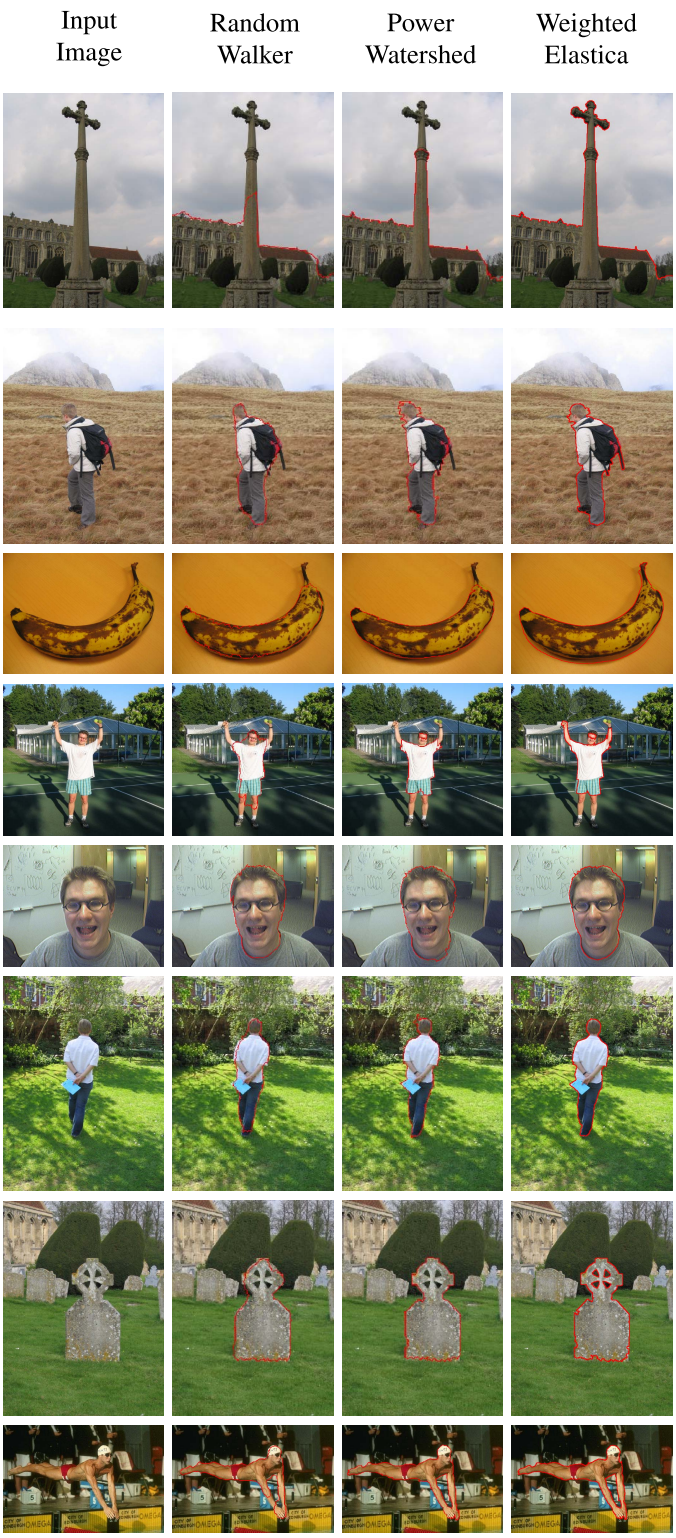

Fig. 10. Sample of the segmentation results of the grab cut data set with the different segmentation methods.

1) Rand Index (RI)
2) Boundary Error (BE)
3) Global Consistency Error(GCE)
4) Variation of Information (VOI)

A good segmentation should have a high Rand index and low boundary error, global consistency error and variation of information. All the images are processed with $\nu = 400$, $\lambda = 50$ and $\beta = \frac{2}{\max(g)}$, where g is the input image. For all the images, QPBO/QPBOP succeeded to provide a complete solution and label all the pixels in our contrast driven elastica method (i.e., a global optimum of the contrast driven elastica model was obtained in each case).

Table I shows the mean results of these segmentation[3] algorithms for the fifty images in the data set. It can be seen that the segmentation obtained by the contrast driven elastica are as good or better than the other algorithms on these images, even though they generally have a fairly strong data term differentiation between the object and the background. Figure 10 show a sample of images and their segmentation results using random walker, power watershed and our weighted elastica model, respectively. In the first four images, we show some of the thin structures where the strength of the curvature model is leveraged, the curvature model can capture much better the top part of the cross, the strap of the backpack, the tip of the banana and the arms of the tennis player. The fifth to the last image feature blob-like structure and illustrate that our model performs as good or better than the remaining methods for such images.

IV. Conclusion

Curvature minimization is a classic regularization model for image segmentation that has received less attention in the past during to the difficulty of optimizing curvature models. The recent advances in introducing efficient formulations and optimization of curvature [1], [6], [10], [25], [26], [31], [34] have revived the research efforts in applying curvature regularization to vision problems such as image segmentation, denoising and inpainting. However, a major challenge associated with minimum boundary curvature models is the segmentation of high curvature structures such as sharp corners and cusps. Previous models such as [11] and [25] associated the curvature regularization with a global data model to help segment such structures. Unfortunately, in practical applications, foreground and background may share the same data profile (*i.e.*, may have the same intensity or texture distributions). In such cases, the curvature segmentation schemes in [11] and [25] would fail to provide an accurate solution. In this paper, we proposed an image segmentation model that weights the curvature locally by the contrast information. We also added the length term to the curvature to complete the formulation of the elastica model originally proposed by Mumford in [20]. The inclusion of the length term allows us to find a global optimum of the model using QPBO/QPBOP in a few seconds.

[3]Some of the results were copied from the original papers of the authors and other were calculated using the authors' implementations and parameters choice to guarantee a fair comparison.

Our quantitative assessment on the GrabCut database shows that our contrast driven elastica model works as good or better than weighted boundary length minimization (Graph Cuts), Random Walker, p-brush and power watershed in the images where the data term provides some discrimination. However, our experiments demonstrate that our model can additionally be used to complete object boundaries in synthetic and real images in which the object/background shared the same appearance, significant parts of the boundary were missing and the target objects possessed an irregular shape. In contrast, other leading algorithms which are known for robust behavior were unable to achieve quality segmentation of these challenging images.

Future work will focus on using more sophisticated appearance terms, extension to 3D segmentation and optimization via parallel processing (e.g., GPUs). Additionally, since our contrast driven elastica provides a general regularization for noisy or ambiguous data, we may be able to apply the contrast driven elastica to other applications in computer vision beyond image segmentation.

Acknowledgment

The authors would like to thanks Dr. Matthias Krueger for providing an executable of his pseudo-elastica algorithm that enabled us to provide an objective comparison in our paper.

References

[1] E. Bae, J. Shi, and X.-C. Tai, "Graph cuts for curvature based image denoising," *IEEE Trans. Image Process.*, vol. 20, no. 5, pp. 1199–1210, May 2011.
[2] X. Bai and G. Sapiro, "A geodesic framework for fast interactive image and video segmentation and matting," in *Proc. ICCV*, Rio de Janeiro, Brazil, 2007, pp. 1–8.
[3] A. Blake, C. Rother, M. Brown, P. Perez, and P. Torr, "Interactive image segmentation using an adaptive GMMRF model," in *Proc. ECCV*, 2004, pp. 428–441.
[4] Y. Boykov and M.-P. Jolly, "Interactive graph cuts for optimal boundary & region segmentation of objects in N-D images," in *Proc. ICCV*, 2001, pp. 105–112.
[5] Y. Boykov and V. Kolmogorov, "Computing geodesics and minimal surfaces via graph cuts," in *Proc. ICCV*, Oct. 2003, pp. 26–33.
[6] A. M. Bruckstein, A. N. Netravali, and T. J. Richardson, "Epi-convergence of discrete elastica," *Appl. Anal.*, vol. 79, nos. 1–2, pp. 137–171, 2001.
[7] V. Caselles, R. Kimmel, and G. Sapiro, "Geodesic active contours," *Int. J. Comput. Vis.*, vol. 22, no. 1, pp. 61–79, 1997.
[8] T. F. Chan and L. A. Vese, "Active contours without edges," *IEEE Trans. Image Process.*, vol. 10, no. 2, pp. 266–277, Feb. 2001.
[9] C. Couprie, L. Grady, L. Najman, and H. Talbot, "Power watershed: A unifying graph-based optimization framework," *IEEE Trans. Pattern Anal. Mach. Intell.*, vol. 33, no. 7, pp. 1384–1399, Jul. 2011.
[10] N. Y. El-Zehiry and L. Grady, "Fast global optimization of curvature," in *Proc. CVPR*, 2010, pp. 3257–3264.
[11] N. El-Zehiry and L. Grady, "Optimization of weighted curvature for image segmentation," *CoRR*, 2010. [Online]. Available: http://arxiv.org/pdf/1006.4175.pdf
[12] S. Esedoglu and J. Shen, "Digital inpainting based on the Mumford–Shah–Euler image model," *Eur. J. Appl. Math.*, vol. 13, no. 4, pp. 353–370, 2002.
[13] G. Funka-Lea *et al.*, "Automatic heart isolation for CT coronary visualization using graph-cuts," in *Proc. ISBI*, Apr. 2006, pp. 614–617.
[14] L. Grady, "Random walks for image segmentation," *IEEE Trans. Pattern Anal. Mach. Intell.*, vol. 28, no. 11, pp. 1768–1783, Nov. 2006.
[15] I. H. Jermyn and H. Ishikawa, "Globally optimal regions and boundaries as minimum ratio weight cycles," *IEEE Trans. Pattern Anal. Mach. Intell.*, vol. 23, no. 10, pp. 1075–1088, Oct. 2001.

[16] M. Kass, A. Witkin, and D. Terzopoulos, "Snakes: Active contour models," *Int. J. Comput. Vis.*, vol. 1, no. 4, pp. 321–331, 1988.
[17] V. Kolmogorov and C. Rother, "Minimizing nonsubmodular functions with graph cuts—A review," *IEEE Trans. Pattern Anal. Mach. Intell.*, vol. 29, no. 7, pp. 1274–1279, Jul. 2007.
[18] V. Kolmogorov and R. Zabin, "What energy functions can be minimized via graph cuts?" *IEEE Trans. Pattern Anal. Mach. Intell.*, vol. 26, no. 2, pp. 147–159, Feb. 2004.
[19] M. Krueger, P. Delmas, and G. Gimel'farb, "Robust and efficient object segmentation using pseudo-elastica," *Pattern Recognit. Lett.*, vol. 34, no. 8, pp. 833–845, 2013. [Online]. Available: http://dx.doi.org/10.1016/j.patrec.2012.12.017
[20] D. Mumford, "Elastica and computer vision," in *Algebraic Geometry and its Applications*. Springer, 1994, pp. 491–506.
[21] C. Nieuwenhuis, E. Töppe, L. Gorelick, O. Veksler, and Y. Boykov, "Efficient squared curvature," in *Proc. IEEE Conf. Comput. Vis. Pattern Recognit. (CVPR)*, Columbus, OH, USA, Jun. 2014, pp. 4098–4105. [Online]. Available: http://dx.doi.org/10.1109/CVPR.2014.522
[22] C. Rother, V. Kolmogorov, and A. Blake, "'GrabCut': Interactive foreground extraction using iterated graph cuts," in *Proc. SIGGRAPH*, 2004, pp. 309–314.
[23] C. Rother, V. Kolmogorov, V. Lempitsky, and M. Szummer, "Optimizing binary MRFs via extended roof duality," in *Proc. CVPR*, 2007, pp. 1–8.
[24] T. Schoenemann and D. Cremers, "Introducing curvature into globally optimal image segmentation: Minimum ratio cycles on product graphs," in *Proc. IEEE 11th ICCV*, Oct. 2007, pp. 1–6.
[25] T. Schoenemann, F. Kahl, and D. Cremers, "Curvature regularity for region-based image segmentation and inpainting: A linear programming relaxation," in *Proc. ICCV*, Kyoto, Japan, 2009, pp. 17–23.
[26] T. Schoenemann, S. Masnou, and D. Cremers, "The elastic ratio: Introducing curvature into ratio-based image segmentation," *IEEE Trans. Image Process.*, vol. 20, no. 9, pp. 2565–2581, Sep. 2011.
[27] J. Shen, S. H. Kang, and T. F. Chan, "Euler's elastica and curvature-based inpainting," *SIAM J. Appl. Math.*, vol. 63, no. 2, pp. 564–592, 2003.
[28] J. Shi and J. Malik, "Normalized cuts and image segmentation," *IEEE Trans. Pattern Anal. Mach. Intell.*, vol. 22, no. 8, pp. 888–905, Aug. 2000.
[29] D. Singaraju, L. Grady, and R. Vidal, "P-brush: Continuous valued MRFs with normed pairwise distributions for image segmentation," in *Proc. CVPR*, Jun. 2009, pp. 1303–1310.
[30] P. Strandmark and F. Kahl, "Curvature regularization for curves and surfaces in a global optimization framework," in *Proc. EMMCVPR*, 2011, pp. 205–218.
[31] X. Tai, J. Hahn, and G. J. Chung, "A fast algorithm for Euler's elastica model using augmented Lagrangian method," *SIAM J. Imag. Sci.*, vol. 4, no. 1, pp. 313–344, 2011. [Online]. Available: http://dx.doi.org/10.1137/100803730
[32] P. Wighton, M. Sadeghi, T. K. Lee, and M. S. Atkins, "A fully automatic random walker segmentation for skin lesions in a supervised setting," in *Proc. MICCAI*, 2009, pp. 1108–1115.
[33] A. Y. Yang, J. Wright, Y. Ma, and S. S. Sastry, "Unsupervised segmentation of natural images via lossy data compression," *Comput. Vis. Image Understand.*, vol. 110, no. 2, pp. 212–225, 2008.
[34] W. Zhu, X. Tai, and T. Chan, "Image segmentation using Euler's elastica as the regularization," *J. Sci. Comput.*, vol. 57, no. 2, pp. 414–438, 2013. [Online]. Available: http://dx.doi.org/10.1007/s10915-013-9710-3

Noha Youssry El-Zehiry received the M.A. degree in mathematics and the Ph.D. degree in computer science from the University of Louisville, in 2006 and 2009, respectively. She is currently a Staff Scientist with Medical Imagining Technologies Team, Siemens Healthcare, Princeton. Her research focuses on image segmentation and pattern recognition, in particular, medical imaging applications. Her interests also include computer vision, machine learning, graph theory, and combinatorial optimization. She has served as a Reviewer for major computer vision and image processing conferences and journals. And one of her biggest passions is the women empowerment in STEM careers.

Leo Grady received the Ph.D. degree from Boston University. He spent nine years with Siemens Corporate Research as a Principal Research Scientist. He has been the Vice President of Research and Development with HeartFlow since 2012. His work has focused on a range of computer vision and medical imaging methods and applications with emphasis on image segmentation and machine learning. He has authored and edited two books on computer vision and data analysis using graph theory, is an Editor of several journals in computer vision and was recently inducted as a fellow of the American Institute of Medical and Biomedical Engineers.